A Random-effects Model for Long-Term Degradation Analysis of Solid Oxide Fuel Cells

Maurizio Guida [a,b], *Fabio Postiglione* [a,*], *Gianpaolo Pulcini* [b]

[a] *Department of Information Engineering, Electrical Engineering and Applied Mathematics (DIEM), University of Salerno, Fisciano (SA), Italy*

[b] *Istituto Motori, National Research Council - CNR, Naples, Italy*

Abstract

Solid oxide fuel cells (SOFCs) are electrochemical devices converting the chemical energy into electricity with high efficiency and low pollutant emissions. Tough very promising, this technology is still in a developing phase, and degradation at the cell/stack level with operating time is still an issue of major concern. Methods to directly observe degradation modes and to measure their evolution over time are difficult to implement, and indirect performance indicators are adopted, typically related to voltage measurements in long-term tests. In order to describe long-term degradation tests, three components of the voltage measurements should be modelled: the smooth decay of voltage over time for each single unit; the variability of voltage decay among units; and the high-frequency small fluctuations of voltage due to experimental noise and lack of fit. In this paper, we propose an empirical random-effects regression model of polynomial type enabling to evaluate separately these three types of variability. Point and interval estimates are also derived for some performance measures, such as the mean voltage, the prediction of cell voltage, the reliability function and the cell-to-cell variability in SOFC stacks. Finally, the proposed methodology is applied to two real case-studies of long-term degradation tests of SOFC stacks.

Keywords: Random effects; Degradation; Reliability estimation; Solid oxide fuel cells.

[*] Corresponding author. *Tel.*: +39 089 962626; *fax*: +39 089 964218. *Email address*: fpostiglione@unisa.it. *Postal address*: Dept. of Information Engineering, Electrical Engineering and Applied Mathematics (DIEM), University of Salerno – Via Giovanni Paolo II, 132 – I-84084 Fisciano (SA) – Italy

Available at: https://doi.org/10.1016/j.ress.2015.03.036

Acronyms

ACF	Autocorrelation Function
AR(q)	Autoregressive of order q
$CoV(x)$	Coefficient of Variation at time x
d.o.f.	degrees of freedom
FGLS	Feasible Generalized Least Squares
GLS	Generalized Least Squares
i.i.d.	independent identically distributed
OLS	Ordinary Least Squares
SOFC	Solid Oxide Fuel Cell

Notation

n; i	number of units; subscript denoting the ith unit
m; j	number of measurements; subscript denoting response and covariates levels for the jth measurement
p	number of parameters in the linear regression model
$\mathbf{x}_j$	$(p \times 1)$ vector of covariate (independent variable) level for the jth measurement, common across units
$\mathbf{X} = \begin{bmatrix} \mathbf{x}_1^T \\ \vdots \\ \mathbf{x}_m^T \end{bmatrix}$	$(m \times p)$ matrix of covariate values at which the m observations are taken
$\mathbf{B}$	$(p \times 1)$ vector of r.v.'s, *i.e.* the coefficients of the linear regression model
$\boldsymbol{\mu}_\mathbf{B}$; $\hat{\boldsymbol{\mu}}_\mathbf{B} = \sum_{1=1}^{n} \hat{\mathbf{B}}_i / n$	$(p \times 1)$ vector of expected value of $\mathbf{B}$; Least Squares estimator
$\boldsymbol{\Sigma}_\mathbf{B}$	$(p \times p)$ covariance matrix of $\mathbf{B}$
$MVN(\boldsymbol{\mu}_\mathbf{B}, \boldsymbol{\Sigma}_\mathbf{B})$	multivariate normal distribution

$\mathbf{B}_i$; $\hat{\mathbf{B}}_i$ ($p \times 1$) vector of r.v.'s containing sampling realization of $\mathbf{B}$ for unit *i*, $\mathbf{B}_i \sim MVN(\boldsymbol{\mu}_B, \boldsymbol{\Sigma}_B)$; Least Squares estimator

ε_{ij} random error on the true response for *i*th unit at $\mathbf{x}_j$

$\sigma^2 = \text{var}[\varepsilon_{ij}]$ unexplained variance in the regression model, common across units

$\boldsymbol{\varepsilon}_i$ ($m \times 1$) noise vector for the *i*th unit, $\boldsymbol{\varepsilon}_i \sim MVN(\mathbf{0}, \boldsymbol{\Omega})$

$\boldsymbol{\Omega}$ ($m \times m$) covariance matrix of $\boldsymbol{\varepsilon}_i$, common across units, $\boldsymbol{\Omega}_i \equiv \boldsymbol{\Omega} = \sigma^2 \mathbf{V}$

$\mathbf{V}$ ($m \times m$) autocorrelation matrix with $V_{jj} = 1$, V_{jj} being the (j, j) entry of the matrix $\mathbf{V}$

$Y_{ij} = \mathbf{B}_i^T \mathbf{x}_j + \varepsilon_{ij}$ response (dependent variable) level for *i*th unit at $\mathbf{x}_j$

$\hat{Y}_{ij} = \hat{\mathbf{B}}_i^T \mathbf{x}_j$ Least Squares estimator of the expected response at $\mathbf{x}_j$ for *i*th unit

$\hat{Y}_j = \hat{\boldsymbol{\mu}}_{\mathbf{B}}^T \mathbf{x}_j$ Least Squares estimator of the mean regression line over the population of items;

$\boldsymbol{\Sigma}_{\hat{\mathbf{B}}|\mathbf{B}}$ ($p \times p$) covariance matrix of $\hat{\mathbf{B}}_i$, given $\mathbf{B}_i = \mathbf{B}$

$\boldsymbol{\Sigma}_{\hat{\mathbf{B}}} = \boldsymbol{\Sigma}_{\mathbf{B}} + E_{\mathbf{B}}\left[\boldsymbol{\Sigma}_{\hat{\mathbf{B}}|\mathbf{B}}\right]$ ($p \times p$) unconditional covariance matrix of $\hat{\mathbf{B}}_i$

1. Introduction

A solid oxide fuel cell (SOFC) is an electrochemical device, which directly converts the chemical energy into electricity with high efficiency and low pollutant emissions. Thus, SOFCs are expected to play a significant role in helping to meet the demand of distributed and stationary power generation systems, provided that high reliability levels are demonstrated by this technology. Indeed, due to high operating temperatures, system components are subjected to significant thermo-mechanical stresses which negatively impact performance and lifetimes. Thus, in the last years a big effort was devoted by industrial companies, universities, and research institutions to improve

understanding of degradation mechanisms, materials and processes in order to extend durability of SOFC systems (typically stacks of serially connected cells).

In particular, degradation at the cell/stack level is an issue of major concern. A number of features affecting cell/stack degradation have been identified which include: electrode contact loss and increased contact resistance, changes in material composition and structure, interdiffusion, phase changes, and deactivation of catalysts [1]. However, methods to directly observe degradation modes and to measure their evolution over time are difficult or even unfeasible to be implemented, and only indirect cell/stack performance indicators are available. Usually, an overall metric of cell/stack degradation is assumed to be the cell/stack output voltage [2], so that typical degradation studies are based on long-term tests where the cell/stack is operated under steady state conditions and the evolution of its voltage over time is measured. These measurements usually contain information about product reliability. In fact, by defining unit failure in terms of the crossing of a specified level of degradation, a time to failure distribution can in principle be derived from the degradation measurements [3].

Available long-term tests on SOFC stacks revealed that different shapes of the cell/stack voltage as a function of time can be observed, as a consequence of technological state of the art and/or operating conditions. In particular, these shapes can be divided into four different types: two shapes with a significant initial drop (wear-in period), followed either by a long-term linear decay during the remainder of operation or by only a short period of linear decay before the degradation becomes progressive in time (wear-out period); and two other shapes where the long-term behaviour is the same as for the previous ones, but the initial drop is absent [4]. Furthermore, when each single cell in a stack is monitored, a variability of the voltage degradation path is often observed across units, as a consequence of lack of uniformity in the manufacturing process and of different operating conditions across units in the stack [5, 6]. This phenomenon appears to be a relevant aspect to be analysed because, in systems comprising groups of stacks, variance in stack characteristics may cause an uneven distribution of load among the stacks which, in turn, may have a negative impact on system

performances and durability [7]. Thus, an index able to measure the lack of uniformity and then this quality component of the manufacturing and the assembly process is identified. Moreover, voltage measures are affected by experimental noise, whose primary sources are measurement errors and temperature, pressure and reactant concentration fluctuations during the tests.

1.1 Problem statement and related works

The purpose of this paper is modelling the degradation phenomenon of SOFC cells in long runs by analysing voltage measurements, in order to estimate some SOFC performance measures, such as the mean voltage, the future degradation growth (measured by predicting cell voltage), the reliability function, and the cell-to-cell variability related to both the manufacturing process and inhomogeneous operating conditions across the stack.

To this aim, three components of the voltage measurements have to be modelled: a) the smooth decay of voltage over time for each single unit; b) the variability of voltage decay among units; and c) the small fluctuations of voltage superimposed on the smooth decay due to experimental noise. It is worth noting that noise characterization can be useful *per se*. For instance, a change in the noise pattern during operating time may be a signature of a specific degradation phenomenon.

Some attempts have been made to evaluate the long-term decay of cell voltage on a physical or electrochemical basis [8, 9], which however fail to satisfactorily reproduce the observed voltage decay over the entire cell life. Degradation phenomena are often analysed by using empirical random-coefficients regression models [3, 10-15] or stochastic processes, e.g. Gamma or Extended Gamma processes [16], in absence of mechanistic models. Indeed, in the field of energy systems, a simple empirical model based on a (linear) polynomial regression approach was introduced in [13] to model battery degradation data to the aim of the online estimation of the state of health of the batteries. However, more sophisticated degradation models can be fruitfully selected on the basis of some physical or chemical models describing the dynamics of the system under analysis, when available. In [14], a (nonlinear) random-effects bi-exponential model was introduced to predict the degradation

rate of membrane electrode assemblies in direct methanol fuel cells, accounting for two heterogeneous degradation characteristics related to the typical chemical reactions and the kinetics of current density in the system. Estimation procedures are performed on some response time series affected by independent identically distributed (henceforth i.i.d.) random errors. A model combining polynomial and exponential functions has been also proposed in [15], focusing on the residual performance of lithium-ion batteries, whose parameters are adjusted online by a particle filter on measurements corrupted by an i.i.d. noise sequence.

1.2 The case studies and the rationale behind the modelling approach

The data sets under analysis are part of a larger data set provided by the Swiss company HEXIS AG to the Consortium of the GENIUS project, a European Community-funded research project, on the diagnosis of SOFC systems. Data refer to two different SOFC systems: an early generation system (henceforth *case study A*) and a subsequent evolution (henceforth *case study B*). Because of industrial reserve reasons, the original voltage and time values have been rescaled in the present paper. Rescaled voltage time series are reported in Fig. 1, together with the corresponding estimated empirical models. Case study A shows some initial drop, while in the case study B the wear-in period is practically absent; in both cases, a long-term almost linear decay is present in most operating time, followed by a wear-out period. A high variability of decay among units is observed, and some superimposed voltage fluctuations are also evident.

In order to analyse voltage data collected in the long-term degradation tests in Fig. 1 and, above all, to compute the reliability function of the SOFC cells composing the stacks, we need a statistical model able to accurately describe not only the linear decay [17] or wear-in period but also the wear-out period, and to handle the variability among the degrading behaviour of the cells, in absence of a physical or electrochemical model of SOFC degradation.

Thus, we propose an empirical random-effects regression model of polynomial type that is sufficiently flexible to describe different behaviours of voltage time series. For further reading on

random-effects regression models and their use in the applications, refer to [18, 19]. However, SOFC systems dynamics is governed by many parameters that are not included in the proposed model, such as temperature, current density, pressure, fuel flow and reactant concentration. These parameters should be kept constant, but typically show small variations during long-term tests, even in the presence of specific controllers. Consequently, we consider that the errors in each voltage path may presumably exhibit an autocorrelated structure. Evidently, the inclusion of the above parameters (if available) in the model could reduce the observed autocorrelation [20, pp. 133-134].

It should be emphasized that the presence of correlated noise in voltage paths makes quite difficult to use the stochastic processes-based degradation models available in the scientific literature, that relies on the assumption of independent increments. For further reading, see [16] and the references within.

We remark that the proposed model proves to be quite "general" because it provides accurate polynomial fitting curves for all of the typical cell voltage degradation paths measured during all the long-term SOFC stacks tests analysed within the GENIUS project, among which we selected the two representative data sets described in this paper. It is worth highlighting that the proposed model enables a separate quantitative evaluation of the variability associated to the cell-to-cell heterogeneity, and the one due to correlated noise: at the best of authors' knowledge, this approach is novel for SOFC system degradation characterization and reliability evaluation.

The paper is organised as follows. Section 2 presents the proposed random-effects model. In Section 3, the main results are provided for point and interval estimation of the model parameters. The evaluation of the future degradation growth, by predicting cell voltage, and the inferential procedure on the reliability function are discussed in Section 4, where a manufacturing quality index is also defined and computed; for sake of clarity, some mathematical details of the aforementioned procedures are included in the Appendices. In Section 5, we check the model assumptions and its limitations. In Section 6, the application to two real case-studies of long-term degradation tests is illustrated and discussed. Finally, in Section 7, we provide some concluding remarks.

2. The model

Let us consider the experimental situation where a *n*-cell stack undergoes a durability test under constant load. For each cell in the stack (which can be viewed as a sample unit randomly selected from a specified population of interest, e.g., a production lot), a sequence of voltage measurements over the operating time is provided. We assume that the observed degradation path of a cell can be viewed as the sum of two components: *i)* a unit-specific (deterministic) function of time, which cannot be observed directly, and *ii)* a random component, usually called "noise". In particular, a polynomial form with unit-specific unknown coefficients is postulated in the present paper for the cell degradation function. Furthermore, it is assumed that the times at which measurements are carried out are pre-specified and noise determinations are possibly correlated across time.

As such, the experimental results are modelled by the linear random-effects regression model

$$Y_{ij} = \mathbf{B}_i^T \ \mathbf{x}_j \ + \ \varepsilon_{ij} \qquad i = 1,...,n; \ \ j = 1,...,m \tag{1}$$

where

- $\mathbf{x}_j = (1, x_j, x_j^2, ..., x_j^{p-1})^T$ is the $(p \times 1)$ vector of the *j*th regressor, with x_j the time (common across units) of the *j*th measurement $(j = 1,...,m)$;
- $\mathbf{B}_i = (B_{i0}, B_{i1}, ..., B_{i(p-1)})^T$ is the $(p \times 1)$ vector of the regression coefficients for the *i*th unit $(i = 1,...,n)$; and
- ε_{ij} is the random noise on the true response for *i*th unit at $\mathbf{x}_j$.

The following distributional assumptions are made for the random terms in the model:

- $\mathbf{B}_i$ and ε_{ij} are independent of each other;
- $\mathbf{B}_i$ are i.i.d. multivariate normal random vectors, $\mathbf{B}_i \sim MVN\left(\boldsymbol{\mu}_B, \boldsymbol{\Sigma}_B\right)$ $(i = 1,...,n)$;

- $\boldsymbol{\varepsilon}_i$, the $(m \times 1)$ noise vector for unit *i*, is multivariate normal, $\boldsymbol{\varepsilon}_i \sim MVN(\mathbf{0}, \boldsymbol{\Omega})$, with a common covariance matrix $\boldsymbol{\Omega}_i \equiv \boldsymbol{\Omega} = \sigma^2 \mathbf{V}$ across units, with $V_{jj} = 1$, V_{jj} being the (j, j) entry of the autocorrelation matrix $\mathbf{V}$.

As a consequence of the above assumptions, it follows that Y_{ij} are normal random variables across each unit *i*, with $Y_{ij} \sim N\left(\boldsymbol{\mu}_{\mathbf{B}}^T \mathbf{x}_j, \mathbf{x}_j^T \boldsymbol{\Sigma}_B \mathbf{x}_j + \sigma^2\right)$, and $\mathrm{Cov}\left[Y_{ij}, Y_{ik}\right] = \mathrm{Cov}\left[\varepsilon_{ij}, \varepsilon_{ik}\right] = \sigma^2 V_{jk}$ $(j, k = 1, ..., m)$. In particular, we assume an autoregressive (AR) model of order *q*, AR(*q*), for the noise $\boldsymbol{\varepsilon}_i$ $(i = 1, ..., n)$ of the *i*th unit defined as

$$\varepsilon_{ij} = \sum_{l=1}^{q} \varphi_l \ \varepsilon_{i,j-l} \ + \ \gamma_{ij}, \tag{2}$$

where $\varphi_1, ..., \varphi_q$ are the AR model parameters, and γ_{ij} is a white noise process with zero mean and variance σ_γ^2. Within model (2), the full noise autocorrelation function is recursively defined by

$$\rho(k) = \sum_{l=1}^{q} \varphi_l \ \rho(k-l) \qquad k = 1, 2, ... \tag{3}$$

where $\rho(k)$ denotes the correlation coefficient between the r.v.'s ε_{ij} and $\varepsilon_{i,j+k}$ $(i = 1, ..., n)$, with $\rho(-k) = \rho(k)$ and $\rho(0) = 1$. Thus, equation (3) completely defines the autocorrelation matrix $\mathbf{V}$.

3. Estimation of model parameters

The proposed regression model contains the unknown quantities $\boldsymbol{\mu}_B$, $\boldsymbol{\Sigma}_B$ and σ^2 which need to be estimated in order to make inference and predictions. Furthermore, the noise autocorrelation matrix $\mathbf{V}$ is usually unknown, and has to be estimated as well. Obviously, the estimation accuracy of the model parameters for the individual paths is affected by the number of observations *m* along each path. In the applications considered in the present paper, *m* is usually very large, so that the sampling variability of the estimates of the model parameters for the individual paths is expected to be small. The estimation accuracy of the distribution of random-effects, instead, is affected by the

number of sample units *n*. The size *n* also influences the accuracy of confidence intervals of model parameters and of functions thereof, such as the reliability function. For the applications here considered *n* is usually small, thus large confidence intervals are to be expected.

The proposed estimation procedure is described by the flow diagram in Fig. 2, and develops according to the following steps:

- estimate, by using the Ordinary Least Squares (OLS) method, the parameters of the degradation model *for each cell voltage time series*, that is, regression coefficients $\mathbf{B}_i$ and the unexplained variance σ^2;
- estimate the noise covariance matrix $\mathbf{\Omega}$ by selecting the most suitable AR(q) model for the noise, represented by the residuals of the OLS procedure;
- estimate the mean vector $\boldsymbol{\mu}_{\mathbf{B}}$ and the unconditional covariance matrix $\boldsymbol{\Sigma}_{\hat{\mathbf{B}}}$ of the OLS estimates of $\mathbf{B}_i$;
- estimate the covariance matrix $\boldsymbol{\Sigma}_{\mathbf{B}}$ of the linear random-effects regression model, possibly using the non-negative definite estimator $\hat{\boldsymbol{\Sigma}}_{\mathbf{B}}^{+}$;
- compute, on the basis of the above estimates, all the quantities of interest.

3.1 Regression coefficients and noise covariance matrix

When noise determinations are i.i.d. r.v.'s, the unknown regression coefficients of each path *i* can be estimated by the OLS method as $\hat{\mathbf{B}}_i = (\mathbf{X}^T\mathbf{X})^{-1}\mathbf{X}^T\mathbf{Y}_i$, where $\mathbf{Y}_i$ is the $(m\times 1)$ vector of *m* degradation measurements for the *i*th unit, and $\mathbf{X}$ is the $(m\times p)$ matrix of the *m* (known) regressor values. It is well known from OLS theory that $\hat{\mathbf{B}}_i$ is an unbiased, multivariate normal, minimum variance linear estimator of $\mathbf{B}_i$, with covariance matrix $\sigma^2(\mathbf{X}^T\mathbf{X})^{-1}$. On the other hand, in case of correlated noise determinations, the Generalized Least Squares (GLS) approach [21] should be used, and parameter estimates should be obtained as $\hat{\mathbf{B}}_i = (\mathbf{X}^T\mathbf{V}^{-1}\mathbf{X})^{-1}\,\mathbf{X}^T\mathbf{V}^{-1}\,\mathbf{Y}_i$ where $\hat{\mathbf{B}}_i$ is still an

unbiased, multivariate asymptotically normal, minimum variance linear estimator, with covariance matrix $\mathbf{\Sigma}_{\hat{\mathbf{B}}|\mathbf{B}} = (\mathbf{X}^T \mathbf{\Omega}^{-1} \mathbf{X})^{-1}$ here assumed to be common across units. When the autocorrelation matrix $\mathbf{V}$ is unknown, the solution for this problem is a Feasible Generalized Least Squares (FGLS) estimation. Such an approach, however, is not easily amenable to the analysis of multiple paths with common noise characteristics. Thus, a different approach is here exploited, which is based on a two-step procedure, where the first step is devoted to obtain model "residuals" by OLS, while the second step exploits these residuals to estimate $\mathbf{V}$, as illustrated below.

It is known that, even in the presence of noise correlation, OLS approach provides point estimates of regression coefficients very close to those computed by GLS, but the sampling variability of these estimates might be seriously underestimated. This suggests using OLS for obtaining point estimates of regression coefficients by $\hat{\mathbf{B}}_i = (\mathbf{X}^T \mathbf{X})^{-1} \mathbf{X}^T \mathbf{Y}_i$. Then, based on the OLS estimates $\hat{\mathbf{B}}_i$, one can obtain an estimate of the mean regression line for the *i*th path by $\hat{Y}_{ij} = \hat{\mathbf{B}}_i^T \mathbf{x}_j$, so that residuals relative to the *i*th path $(i = 1,...,n)$ can be obtained as

$$e_{ij} = Y_{ij} - \hat{Y}_{ij} \qquad j = 1,...,m. \tag{4}$$

Residuals (4) are then used to obtain a least square estimate of the noise correlation coefficients $\hat{\varphi}_l$ $(l = 1,...,q)$ in (2), by applying the OLS approach to the *n* computed noise sample paths, considered as independent realizations of a same noise process. The order *q* of the autoregressive model is derived by applying a stepwise procedure based on *F*-tests [22] to the linear regression model (2). Finally, the noise autocorrelation AR(*q*) function is obtained as

$$r(k) = \sum_{l=1}^{q} \hat{\varphi}_l \, r(k-l) \qquad k = 1,...,m \tag{5}$$

by solving the first *q* linear equations from (5), taking into account that $r(-k) = r(k)$ and $r(0) = 1$. Thus, the symmetric Toeplitz matrix $\hat{\mathbf{V}}$ generated by the $r(k)$ in (5) provides an estimate of the autocorrelation matrix $\mathbf{V}$.

A minimum variance estimate of σ^2 relative to the *i*th path is obtained by

$$s_i^2 = \frac{\sum_{j=1}^{m} e_{ij}^2}{m-p}, \tag{6}$$

and a more precise estimate of σ^2 can be computed by pooling the individual estimates s_i^2 $(i = 1,...,n)$ by

$$s^2 = (1/n)\sum_{i=1}^{n} s_i^2 . \tag{7}$$

An estimate of the covariance matrix $\mathbf{\Omega}$ can then be obtained as

$$\hat{\mathbf{\Omega}} = s^2 \hat{\mathbf{V}} . \tag{8}$$

Since *m* is large in the present application, in the following we will develop the estimation procedures as if the noise covariance matrix $\mathbf{\Omega} = \sigma^2 \mathbf{V}$ were known and equal to $\hat{\mathbf{\Omega}}$.

3.2 Expected regression coefficients and random-effects variability

Given $\mathbf{B}_i$, GLS theory states that $\hat{\mathbf{B}}_i \sim MVN\left(\mathbf{B}_i, \mathbf{\Sigma}_{\hat{\mathbf{B}}|\mathbf{B}} = (\mathbf{X}^T \mathbf{\Omega}^{-1} \mathbf{X})^{-1}\right)$. Thus, it follows that $\hat{Y}_{ij} \sim N\left(\mathbf{B}_i^T \mathbf{x}_j, \mathbf{x}_j^T \mathbf{\Sigma}_{\hat{\mathbf{B}}|\mathbf{B}} \mathbf{x}_j\right)$. It is worth noting that, taking the variability due to random-effects into account, the "unconditional" distribution of $\hat{\mathbf{B}}_i$ is still multivariate normal, with mean $\mathbf{\mu}_B$ and covariance matrix $\mathbf{\Sigma}_{\hat{\mathbf{B}}} = \mathbf{\Sigma}_{\mathbf{B}} + \mathbf{\Sigma}_{\hat{\mathbf{B}}|\mathbf{B}}$ (for the details, see Appendix A).

On the basis of the estimates $\hat{\mathbf{B}}_i$ $(i = 1,...,n)$ relative to *n* observed paths, a minimum variance linear estimator of $\mathbf{\mu}_B$ is obtained as

$$\hat{\mathbf{\mu}}_{\mathbf{B}} = \frac{\sum_{i=1}^{n} \hat{\mathbf{B}}_i}{n}, \tag{9}$$

which is a multivariate normal random vector with mean $\boldsymbol{\mu}_{\mathbf{B}}$ and covariance matrix $(1/n)\boldsymbol{\Sigma}_{\hat{\mathbf{B}}}$. A minimum variance point estimate of the mean regression line over the population of items is then given by $\hat{Y}_j = \hat{\boldsymbol{\mu}}_{\mathbf{B}}^T \mathbf{x}_j$, which is a normal r.v. with mean $\boldsymbol{\mu}_{\mathbf{B}}^T \mathbf{x}_j$ and variance $(1/n)\mathbf{x}_j^T \boldsymbol{\Sigma}_{\hat{\mathbf{B}}} \mathbf{x}_j$.

In order to estimate the unknown covariance matrix $\boldsymbol{\Sigma}_{\mathbf{B}}$, it can be observed that $\boldsymbol{\Sigma}_{\mathbf{B}} = \boldsymbol{\Sigma}_{\hat{\mathbf{B}}} - \boldsymbol{\Sigma}_{\hat{\mathbf{B}}|\mathbf{B}}$, where $\boldsymbol{\Sigma}_{\hat{\mathbf{B}}}$ can be estimated by

$$\hat{\boldsymbol{\Sigma}}_{\hat{\mathbf{B}}} = \frac{1}{n-1} \sum_{i=1}^{n} \left[\hat{\mathbf{B}}_i - \hat{\boldsymbol{\mu}}_{\mathbf{B}} \right] \left[\hat{\mathbf{B}}_i - \hat{\boldsymbol{\mu}}_{\mathbf{B}} \right]^T, \tag{10}$$

while $\boldsymbol{\Sigma}_{\hat{\mathbf{B}}|\mathbf{B}}$ is estimated by $(\mathbf{X}^T \hat{\boldsymbol{\Omega}}^{-1} \mathbf{X})^{-1}$, thus obtaining

$$\hat{\boldsymbol{\Sigma}}_{\mathbf{B}} = \hat{\boldsymbol{\Sigma}}_{\hat{\mathbf{B}}} - (\mathbf{X}^T \hat{\boldsymbol{\Omega}}^{-1} \mathbf{X})^{-1}. \tag{11}$$

Note that, due to sampling fluctuations, the matrix $\hat{\boldsymbol{\Sigma}}_{\mathbf{B}}$ may not always be non-negative definite, which would be incompatible with a covariance matrix. In such a case, one can resort to the procedure proposed in [23], also suggested in [3], which defines a modified non-negative definite estimator for $\boldsymbol{\Sigma}_{\mathbf{B}}$. This estimator is obtained by decomposing $\hat{\boldsymbol{\Sigma}}_{\mathbf{B}}$ as the sum of a non-negative definite matrix $\hat{\boldsymbol{\Sigma}}_{\mathbf{B}}^{+}$ and a negative definite matrix $\hat{\boldsymbol{\Sigma}}_{\mathbf{B}}^{-}$. Therefore, $\hat{\boldsymbol{\Sigma}}_{\mathbf{B}}^{+}$ can be interpreted as the non-negative definite matrix closest to $\hat{\boldsymbol{\Sigma}}_{\mathbf{B}}$, and used as an estimator for $\boldsymbol{\Sigma}_{\mathbf{B}}$.

3.3 Confidence interval for mean cell voltage

An interval estimate of the mean level of voltage at time x_j over the population of cells can be obtained by considering that the r.v. $W = \left(\hat{Y}_j - \boldsymbol{\mu}_{\mathbf{B}}^T \mathbf{x}_j \right) / s_{\hat{Y}_j}$, where $s_{\hat{Y}_j} = \sqrt{(1/n)\, \mathbf{x}_j^T \hat{\boldsymbol{\Sigma}}_{\hat{\mathbf{B}}} \mathbf{x}_j}$, is distributed as a Student r.v. with $\nu = n-1$ degrees of freedom (d.o.f.). Thus, an equal-tailed $(1-\alpha)$ confidence interval for the population mean can be obtained as

$$\hat{\boldsymbol{\mu}}_{\mathbf{B}}^T \mathbf{x}_j \pm t_{1-\alpha/2;n-1} \sqrt{(1/n)\, \mathbf{x}_j^T \hat{\boldsymbol{\Sigma}}_{\hat{\mathbf{B}}} \mathbf{x}_j}, \tag{12}$$

where $t_{1-\alpha/2;n-1}$ is the $(1-\alpha/2)$-quantile of the Student distribution with $\nu = n-1$ d.o.f.

4. Inference on performance and manufacturing quality measures

In this Section, on the basis of the estimates of the model parameters, some measures of the SOFCs performances, namely the future degradation growth, the reliability function, and an index of the manufacturing process, say the cell-to-cell variability, are estimated.

4.1 Prediction of cell voltage

Prediction intervals for the degradation level at future time x of a generic item of the population can be quite useful in discriminating anomalous situations from normal ones, because measured voltage levels lower than the predicted ones can denote a sudden acceleration of the degradation process.

Let $\hat{Y}_x$ be an estimate of the mean voltage level at time x, based on *n* voltage degradation paths with *m* observations each, given by $\hat{Y}_x = \hat{\boldsymbol{\mu}}_{\mathbf{B}}^T \mathbf{x}$. Using this estimate, we can construct a prediction interval that contains with assigned probability $1-\alpha$ the voltage level Y_x at time x of an item randomly selected from the population of interest. To this aim, consider that the random variable $Y_x - \hat{Y}_x$ is normally distributed with zero mean and variance given by

$$\sigma^2_{Y_x-\hat{Y}_x} = \mathbf{x}^T \boldsymbol{\Sigma}_{\mathbf{B}} \mathbf{x} + \sigma^2 + (1/n)\mathbf{x}^T \boldsymbol{\Sigma}_{\hat{\mathbf{B}}} \mathbf{x}. \tag{13}$$

Thus $Z = \left(Y_x - \hat{Y}_x\right)/\sigma_{Y_x-\hat{Y}_x}$ is a standard normal variable and a prediction interval for Y_x is defined by

$$\Pr\left\{\hat{Y}_x - z_{1-\alpha/2}\sigma_{Y_x-\hat{Y}_x} < Y_x < \hat{Y}_x + z_{1-\alpha/2}\sigma_{Y_x-\hat{Y}_x}\right\} = 1-\alpha, \tag{14}$$

where $z_{1-\alpha/2}$ is the $(1-\alpha/2)$-quantile of the standard normal distribution. This interval takes into account both the variability due to the random-effects and the variability due to the uncertainty in the

estimate. Obviously, this interval has a probability content exactly equal to $(1-\alpha)$ only when all of the parameters involved in the term $\sigma_{Y_x-\hat{Y}_x}$ are *known*. When the unknown parameters are substituted by their estimates, the probability content is only approximately equal to $(1-\alpha)$, although the theoretical value is asymptotically attained. In such a case, a conservative interval may be computed by using the $(1-\alpha/2)$-quantile of the Student distribution with $\nu = n-1$ degrees of freedom in place of $z_{1-\alpha/2}$. Note that, only the lower bound of the prediction interval is usually of interest in the present application, as the aim is to detect anomalous *low* levels of the voltage, due to a sudden acceleration of the degradation process.

4.2 Reliability function

Let $Y(x) = \mathbf{B}^T\mathbf{x}$ denote the voltage level at time x (in absence of noise) of a cell randomly selected in the population. Under the assumptions made on the random-effects regression model (1), $Y(x)$ is a normally distributed r.v. with mean $\boldsymbol{\mu}_{\mathbf{B}}^T\mathbf{x}$ and variance $\mathbf{x}^T\boldsymbol{\Sigma}_{\mathbf{B}}\mathbf{x}$.

Then, given the lowest acceptable level for the cell voltage $y_{\lim}$, under the model assumptions, the reliability function at time x can be defined as

$$R(x) = \Pr\{Y(x) > y_{\lim}\} = \Phi\left[\frac{\boldsymbol{\mu}_{\mathbf{B}}^T\mathbf{x} - y_{\lim}}{\sqrt{\mathbf{x}^T\boldsymbol{\Sigma}_{\mathbf{B}}\mathbf{x}}}\right], \tag{15}$$

where $\Phi(\cdot)$ is the standard normal cumulative distribution function. A point estimate of $R(x)$ is given by

$$\hat{R}(x) = \Phi\left[\frac{\hat{\boldsymbol{\mu}}_{\mathbf{B}}^T\mathbf{x} - y_{\lim}}{\sqrt{\mathbf{x}^T\hat{\boldsymbol{\Sigma}}_{\mathbf{B}}\mathbf{x}}}\right]. \tag{16}$$

A procedure to compute an approximate confidence interval on the true reliability $R(x)$ is derived, and is presented and discussed in Appendix B.

4.3 Cell-to-cell variability

Recalling that voltage $Y(x)$ of a cell, in absence of noise, is normally distributed with mean $\boldsymbol{\mu}_{\mathbf{B}}^{T}\,\mathbf{x}$ and variance $\mathbf{x}^{T}\boldsymbol{\Sigma}_{\mathbf{B}}\mathbf{x}$, a convenient measure of cell-to-cell variability at time x appears to be the coefficient of variation $CoV(x)=\sqrt{\mathbf{x}^{T}\boldsymbol{\Sigma}_{\mathbf{B}}\mathbf{x}}\,/\,\boldsymbol{\mu}_{\mathbf{B}}^{T}\mathbf{x}$. As already remarked, the variability of the voltage of the cells composing a stack are related to a lack of uniformity in the cell manufacturing process and to different operating conditions across units in the stack. The lower $CoV(x)$, the higher the quality of the SOFC system. Since $\boldsymbol{\Sigma}_{\mathbf{B}}$ and $\boldsymbol{\mu}_{\mathbf{B}}$ are not known, the estimator

$$\hat{C}oV(x)=\sqrt{\mathbf{x}^{T}\hat{\boldsymbol{\Sigma}}_{\mathbf{B}}\mathbf{x}}\,/\,\hat{\boldsymbol{\mu}}_{\mathbf{B}}^{T}\mathbf{x} \tag{17}$$

can be used in place of the true value.

5. Checking model assumptions and limitations

In principle, the best way to describe long-term degradation of cell voltage would be to use a physical-driven model based on the underlying physical and/or electrochemical mechanisms originating this phenomenon. As previously pointed out, however, this approach is presently unfeasible, so that in order to describe the long-term degradation behaviour of a cell one has to resort to empirical-based models. Due to their non-mechanistic nature, however, empirical models are possibly subjected to drawbacks, so that we will discuss below under what constraints the polynomial regression model (1) is consistent with the degradation phenomenon of cell voltage.

The first problem to be addressed is how establishing the degree of the polynomial model (1) in practical applications. From a purely statistical point of view, this problem can be solved by using a stepwise procedure, where an *F*-test is sequentially carried out by entering additional terms of increasing order until the null hypothesis that the current coefficient is zero cannot be rejected. It is to be noted, however, that an uncritical use of this procedure may produce results with no physical meaning. In particular, a large preliminary analysis based on many data sets pertaining to different

cell prototypes, has shown that, in case of polynomials of order greater than 3, same-order coefficients relative to some cells in a same stack or to cells in different stacks are not statistically significant or even have different sign.

This suggests that coefficients of order higher than 3 are not conveying information on common features of the underlying degradation phenomenon, but rather contribute to adjusting the polynomial model to some local variations along a specific path. Thus, polynomial models of order higher than 3 can have no physical meaning in such an application. On the other hand, the third-order polynomial model, although very simple and straightforward, has proved to be sufficiently flexible to accurately describe the cell voltage behaviour over time, in presence of all of the shapes usually observed for this technological item. At the same time, it has proved to be a model with a very stable behaviour of its coefficients. In particular, very high coefficients of determination R^2 (usually greater than 0.99, and never smaller than 0.95) have been observed for all of the analysed data sets. Moreover, for all of the cells in a same stack, and for all of the different prototypes analysed, the same-order coefficients had the same sign (B_{i0} and B_{i2} being always positive, while B_{i1} and B_{i3} being always negative, for each cell *i*) and, when viewed as random variables over the cell population, these coefficients showed marginal probability distributions concentrated around their mean values. As such, in this paper we will assume that the voltage degradation of the cell *i* over time in absence of noise, say $Y_i(x) = \mathbf{B}_i^T \mathbf{x}$, is described by a third-order polynomial, i.e. $p = 4$.

Another relevant aspect to be considered is that, while the observed instantaneous voltage is non-monotone over time (as a consequence of the small fluctuations due to random variations of temperature, pressure and reactant concentration), the actual voltage should reasonably be a monotone decreasing function over time. As previously discussed, the degradation process $Y(x) = \mathbf{B}^T \mathbf{x}$ is here modelled by a third-order polynomial function with $\mathbf{B}$ being a four-dimensional random vector distributed according to a *MVN* distribution. Since, however, a third-order polynomial is not constrained to be a monotone decreasing function for all values of $\mathbf{B}$, it is necessary to check

whether the *estimated MVN* distribution of $\mathbf{B}$ is compatible with the monotonicity assumption. From a practical point of view, this requires to check whether, under the estimated *MVN* distribution, the probability of observing a $\mathbf{B}$ vector not in keeping with the monotonicity assumption is *negligible*. To this aim, it can be readily shown that a third-order polynomial is monotone decreasing if and only if the model parameters B_1, B_2 and B_3 satisfy the constraint $B_2^2 - 3B_1B_3 < 0$. Thus, once the parameters of the *MVN* distribution of $\mathbf{B}$ have been estimated, a Monte Carlo simulation method can be used to check whether the fraction of the $\mathbf{B}$ vectors not satisfying the monotonicity constraint is actually negligible.

Finally, a further model assumption is that the noise vector for each cell is *MVN*, with an autoregressive structure as in (2). This assumption implies that the γ_{ij} in (2) are i.i.d. normal variables with zero mean. Thus, a check of normality of the γ_{ij} can be readily made by a graphical tool such as the normal probability plot, and/or applying a formal statistical test such as the Lilliefors test. Then, the independence assumption can be checked by calculating the autocorrelation function of the γ_{ij} for each cell *i*.

6. Case studies data analysis

To the aim of illustrating the proposed methodology, we analyse two different data sets corresponding to two different SOFC systems: an early generation system (*case study A*) and a subsequent evolution (*case study B*), as already remarked in Section 1.2.

The routines for data analysis have been implemented using the R language [24] and the IMSL Fortran Libraries. For each data set, the overall execution time of the computer code that estimates model parameters and all quantities of interest is less than 1 second on a notebook based on an Intel® Core™ i7-2620M CPU @ 2.70 GHz, which shows that the proposed degradation model and estimation procedure are easy to apply.

6.1 Case study A

The data set consists of independent measurements, taken at $m = 288$ constant time intervals, of the voltage of $n = 5$ cells forming a stack, during a long-term test operated under constant load conditions [6]. For each cell under study, Fig. 1(a) depicts the observed (rescaled) voltage as a function of (rescaled) time: after a very smooth initial drop of voltage, a short period of quasi-linear behaviour follows, and then the degradation becomes progressive in time. One of the five cells, namely the cell no. 5, however, started to drift substantially at about 2/3 of total test time, and then it will not be considered in the following analyses.

By assuming a third-order polynomial empirical model as deterministic component of the degradation path, the regression lines for the cells no. 1-4 were obtained on the basis of the OLS method, and are shown in Fig. 1(a). The estimates of the regression coefficients, their sampling mean and standard deviation, and the coefficients of determination are given in Table 1. Based on the point estimates of the regression coefficients, the estimate of the (unconditional) covariance matrix $\boldsymbol{\Sigma}_{\hat{\mathbf{B}}}$, defined by (10), was computed and is shown below

$$\hat{\boldsymbol{\Sigma}}_{\hat{\mathbf{B}}} = \begin{vmatrix} 3.17294\text{E-}06 & & & \\ -2.47318\text{E-}06 & 3.56147\text{E-}05 & & \\ 3.81697\text{E-}06 & -1.06814\text{E-}04 & 3.70663\text{E-}04 & \\ 4.94123\text{E-}06 & 7.97576\text{E-}05 & -3.10248\text{E-}04 & 2.89543\text{E-}04 \end{vmatrix} \tag{18}$$

A visual check from Fig. 1(a), and the values of R^2 coefficients ranging between 0.993 and 0.997, clearly shows that a third-order polynomial curve represents an accurate empirical model for the deterministic component of voltage degradation with time.

Then, on the basis of the estimated regression line for each cell, residuals $e_{i,j}$ ($i = 1,...,4$ $j = 1,...,m$) are obtained by (4), and the noise autocorrelation function (ACF) [21] is calculated by (5). According to the approach described in Section 3.1, the order of the noise AR(q) correlation model was found to be $q = 4$. Figure 3(a) shows the averaged sample noise ACF, obtained by averaging the individual sample ACF's over the four paths, and the noise AR(4) ACF. This model seems to fit well the observed noise autocorrelation, and observations appear to be practically

uncorrelated from a time lag of about 30 time units. In Table 2 the estimates of the noise variance of the *i*th path are given, along with the pooled estimate $s^2 = 1.57495E-07$.

Then, the covariance matrix $\mathbf{\Omega}$ was estimated by (8), which in turn allows to estimate the (conditional) covariance matrix $\mathbf{\Sigma}_{\hat{\mathbf{B}}|\mathbf{B}}$ by $(\mathbf{X}^T\hat{\mathbf{\Omega}}^{-1}\mathbf{X})^{-1}$, viz.

$$\hat{\mathbf{\Sigma}}_{\hat{\mathbf{B}}|\mathbf{B}} = \begin{vmatrix} 7.96622E\text{-}08 & & & \\ -5.93644E\text{-}07 & 6.60323E\text{-}06 & & \\ 1.20405E\text{-}06 & -1.55011E\text{-}05 & 3.92351E\text{-}05 & \\ -7.11100E\text{-}07 & 9.92951E\text{-}05 & -2.63248E\text{-}05 & 1.82178E\text{-}05 \end{vmatrix} \tag{19}$$

The comparison of the estimates $\hat{\mathbf{\Sigma}}_{\hat{\mathbf{B}}}$ and $\hat{\mathbf{\Sigma}}_{\hat{\mathbf{B}}|\mathbf{B}}$ shows that the unconditional variability of the regression coefficients is about one order of magnitude larger than the conditional one, that is, the observed variability of these coefficients is much larger than their (estimated) theoretical sampling variability. This is a clear indication of the presence of random-effects, and then cells cannot be treated as exchangeable items. From (11), the estimate of the random-effects covariance matrix $\mathbf{\Sigma}_{\mathbf{B}}$ is obtained and is given below

$$\hat{\mathbf{\Sigma}}_{\mathbf{B}} = \begin{vmatrix} 3.09328E\text{-}06 & & & \\ -1.87631E\text{-}06 & 2.90114E\text{-}05 & & \\ 2.61292E\text{-}06 & -9.13143E\text{-}05 & 3.31428E\text{-}04 & \\ 5.65233E\text{-}06 & 6.98281E\text{-}05 & -2.83923E\text{-}04 & 2.71325E\text{-}04 \end{vmatrix} \tag{20}$$

This matrix, however, is not positive definite, so that the positive definite matrix $\hat{\mathbf{\Sigma}}_{\mathbf{B}}^{+}$ closest to (20) was obtained. It results that the matrix $\hat{\mathbf{\Sigma}}_{\mathbf{B}}^{+}$ coincides in practice with matrix (18). Thus, in the following we will assume $\hat{\mathbf{\Sigma}}_{\mathbf{B}}^{+} = \hat{\mathbf{\Sigma}}_{\hat{\mathbf{B}}}$.

In order to check the model assumptions, the Normal probability plot and the estimated ACF of the residuals γ_i defined in (2), are computed. In particular, for cell no. 1, plots of these quantities are given in Figs. 4(a) and 5(a), respectively. From this figures, and from similar results (not reported here for sake of space) obtained for the other cells, it appears that the assumption of a white noise for γ_i can be reasonably accepted. Moreover, by using Monte Carlo simulation, it was found that the

fraction of $\mathbf{B}$ vectors in the estimated *MVN* distribution that do not satisfy the monotonicity assumption is less than 0.14%.

On the basis of the estimates $\hat{\boldsymbol{\mu}}_{\mathbf{B}}$ in Table 1 and $\hat{\boldsymbol{\Sigma}}_{\hat{\mathbf{B}}}$ in (18), a confidence interval on the true mean voltage of cell population can be obtained by using (12). In particular, Fig. 6(a) shows the 90% confidence interval for the mean.

An unconditional prediction interval with an approximate $(1-\alpha)$ probability content for the observed voltage of a cell can be obtained by (13) and (14). In particular, Fig. 6(a) also shows the prediction interval with an approximate 90% probability level computed by using the Student quantiles. As previously observed, only the lower bound of the prediction interval is actually of practical interest for monitoring anomalous cell behaviours.

6.2 Case study B

The second data set here analysed refers to a more advanced system and consists of independent measurements, taken at $m = 233$ constant time intervals, of the voltage of $n = 5$ cells forming a stack, during a long-term test operated under constant load conditions. For each cell under study, Fig. 1(b) depicts the observed (rescaled) voltage as a function of (rescaled) time, in the same time units as for the case study A. From the figure it appears that the voltage shape is qualitatively similar to the that of cells of case study A.

In line with case study A analysis, we assume a third-order polynomial empirical model as deterministic component of the degradation path. Figure 1(b) shows the five observed voltage paths along with the estimated regression lines, computed by the OLS method. The point estimates of regression coefficients, their sampling means and standard deviations over the five cells sample, and the coefficients of determination R^2 are given in Table 3.

The estimate of the covariance matrix $\boldsymbol{\Sigma}_{\hat{\mathbf{B}}}$, defined by (10), is shown below

| 1.33839E-06 |

$$\hat{\boldsymbol{\Sigma}}_{\hat{\mathbf{B}}} = \begin{vmatrix} \text{-5.61395E-07} & \text{5.50015E-05} & & \\ \text{-1.24443E-06} & \text{-1.41958E-04} & \text{3.96480E-04} & \\ \text{1.79380E-06} & \text{1.03135E-04} & \text{-2.92747E-04} & \text{2.18049E-04} \end{vmatrix} \tag{21}$$

After checking Fig. 1(b) and the values of R^2 coefficients, ranging between 0.954 and 0.979, it appears that a third-order polynomial function represents a satisfactory empirical model for voltage degradation with time, for the case study B too.

On the basis of the estimated regression line for each cell, residuals $e_{i,j}$ ($i = 1,...,5;\ j = 1,...,m$) are obtained by (4), and the noise ACF is calculated by (5). According to the approach described in Section 3.1, the order of the noise correlation AR(q) model is $q = 3$ for the data set of case study B. Figure 3(b) shows the averaged sample noise ACF, obtained by averaging the individual sample ACF's over the five paths, and the noise AR(3) ACF. In this case the autocorrelation among noise observations appears to be sensibly lower than in case study A. Indeed, noise observations appears to be practically uncorrelated after a time interval which is three times smaller than that of case study A. Table 4 reports the pooled estimate of noise variance $s^2 = 3.10481E-07$, resulting about two times the noise variance of case study A.

Then, an estimate $\hat{\boldsymbol{\Omega}}$ of the covariance matrix $\boldsymbol{\Omega}$ is obtained, which in turn allows to estimate the covariance matrix $\boldsymbol{\Sigma}_{\hat{\mathbf{B}}|\mathbf{B}}$ by $(\mathbf{X}^T\hat{\boldsymbol{\Omega}}^{-1}\mathbf{X})^{-1}$, reported below

$$\hat{\boldsymbol{\Sigma}}_{\hat{\mathbf{B}}|\mathbf{B}} = \begin{vmatrix} \text{9.38623E-08} & & & \\ \text{-8.93644E-07} & \text{1.17090E-05} & & \\ \text{2.27214E-06} & \text{-3.38453E-05} & \text{1.04720E-04} & \\ \text{-1.68593E-06} & \text{2.69272E-05} & \text{-8.69397E-05} & \text{7.43075E-05} \end{vmatrix} \tag{22}$$

The comparison of the estimates $\hat{\boldsymbol{\Sigma}}_{\hat{\mathbf{B}}}$ and $\hat{\boldsymbol{\Sigma}}_{\hat{\mathbf{B}}|\mathbf{B}}$ shows again that the unconditional variability of regression coefficients is much larger than the conditional one, thus indicating that a random effect should be present and cells cannot be treated as exchangeable items in this case, too. From (11), the estimate of the covariance matrix of random-effects $\boldsymbol{\Sigma}_{\mathbf{B}}$ is obtained and is given below

$$\begin{vmatrix} \text{1.24453E-06} \end{vmatrix}$$

$$\hat{\boldsymbol{\Sigma}}_{\mathbf{B}} = \begin{vmatrix} 3.32249\text{E-}07 & 4.32925\text{E-}05 & & \\ -3.51657\text{E-}06 & -1.08113\text{E-}04 & 2.91760\text{E-}04 & \\ 3.47972\text{E-}06 & 7.62078\text{E-}05 & -2.05807\text{E-}04 & 1.43741\text{E-}04 \end{vmatrix} \tag{23}$$

Again, this matrix is not positive definite, so that the positive definite matrix $\hat{\boldsymbol{\Sigma}}_{\mathbf{B}}^{+}$ closest to (23) is obtained and is reported below

$$\hat{\boldsymbol{\Sigma}}_{\mathbf{B}}^{+} = \begin{vmatrix} 1.33694\text{E-}06 & & & \\ -5.21717\text{E-}07 & 5.39212\text{E-}05 & & \\ -1.40880\text{E-}06 & -1.37482\text{E-}04 & 3.77940\text{E-}04 & \\ 1.95584\text{E-}06 & 9.87232\text{E-}05 & -2.74470\text{E-}04 & 2.00031\text{E-}04 \end{vmatrix} \tag{24}$$

In order to check the model assumptions, the Normal probability plot and the estimated ACF of the residuals γ_i defined in (2), are computed. In particular, for cell no. 2, plots of these quantities are given in Figs. 4(b) and 5(b), respectively. From these figures, and from similar results (not reported here for sake of space) obtained for the other cells, it appears that the assumption of a white noise for γ_i can be reasonably accepted in this case, too. Moreover, by using Monte Carlo simulations, it was found that the fraction of $\mathbf{B}$ vectors in the estimated *MVN* distribution that do not satisfy the monotonicity assumption is about 1.8%.

On the basis of the estimates $\hat{\boldsymbol{\mu}}_{\mathbf{B}}$ in Table 3 and $\hat{\boldsymbol{\Sigma}}_{\hat{\mathbf{B}}}$ in (21), a confidence interval for the true mean voltage of cell population can be obtained by using (12). In particular, Fig. 6(b) shows the 90% confidence interval for the mean. An unconditional prediction interval with an approximate $(1-\alpha)$ probability level for the observed voltage of a cell can be obtained by (13) and (14). In particular, Fig. 6(b) also shows the (approximated) 90% prediction interval computed by using the Student quantiles, pointing out that for case study B both these intervals are significantly narrower than the corresponding intervals for case study A.

6.3 Comparison of reliability and cell-to-cell variability of A and B prototypes

As pointed out at the beginning of Section 6, case studies A and B refer to two different SOFC

systems, case study B regarding a subsequent generation system whose degradation should be supposedly slower and whose reliability should be accordingly higher. In Fig. 7, we have then compared the reliability function of the two systems (both in terms of point estimate and of 90% lower confidence limit), by assuming as voltage threshold $y_{\lim} = 0.95 \times Y(0)$, $Y(0)$ being the mean voltage level of each system at time zero. As expected, the reliability of the next generation system is significantly higher.

By using (17), the coefficient of variation of the random variable $Y(x)$ with respect to random-effects is calculated and presented in Fig. 8. It results that this manufacturing quality index for the system A tends to increase with time, from an initial value of about 1% to more than 3% at the end of the test. On the contrary, the coefficient of variation of System B remains quite stable during the operating time, going from an initial value of about 0.6% to about 0.9% at the end of the test, thus clearly demonstrating a significantly better quality of the next generation stack.

7. Conclusions

In the present paper a random-effects regression model of polynomial type has been proposed for describing the main components of variability observed in long-term SOFC degradation tests, operated under steady state conditions. Indeed, experimental experience has shown that these components are: voltage decay over time for each single cell, voltage variability among cells, and noise variability. Point and interval estimates of regression model parameters and reliability function have been derived, and a method based on the coefficient of variation for measuring the manufacturing quality of SOFC stacks have been presented. Then, the methodology has been applied to two real case studies of SOFC systems belonging to different prototype generations. The proposed approach turns out to be computational efficient and able to quantitatively assess performance variability of a SOFC system in terms of durability and cell-to-cell variability. It can be also useful for a comparison between different SOFC systems.

Further improvements to the proposed model could be derived by including other variables influencing the SOFC stack dynamics, in particular temperature and current flowing in the system, whose fluctuations influence (almost) contemporarily all the cells of the stack.

Acknowledgement

The authors thank Dr. Boris Iwanschitz (on leave from HEXIS AG) and Dr. Andreas Mai (HEXIS AG) for having provided the data sets analysed in this paper and for their fruitful comments. This work was carried out in part in the framework of the projects GENIUS (Generic diagnosis instrument for SOFC systems) and DESIGN (Degradation signatures identification for stack operation diagnostics), both funded by European Community's Seventh Framework Programme (FP7/2007-2013) for the Fuel Cells and Hydrogen Joint Technology Initiative under grant agreements n° 245128 and n° 256693, respectively.

References

[1] Steinberger-Wilckens R, Blum L, Buchkremer H-P, Gross S, de Haart LGJ, Hilpert K, et al. Overview of the development of solid oxide fuel cells at Forschungszentrum Juelich. International Journal of Applied Ceramic Technology 2006;3:470–6.

[2] Gemmen RS, Williams MC, Gerdes K. Degradation measurement and analysis for cells and stacks. Journal of Power Sources 2008;184:251–9.

[3] Lu CJ and Meeker WQ. Using degradation measures to estimate a time-to-failure distribution. Technometrics 1993;35:161–174.

[4] de Haart LGJ, Mougin J, Posdziech O, Kiviaho J, Menzler NH. Stack degradation in dependence of operation parameters; the Real-SOFC sensitivity analysis. Fuel Cells 2009;9:794–804.

[5] Christiansen N, Kristensen S, Holm-Larsen H. Status of the SOFC development at Haldor Topsøe/Risø. Proceedings of 8th International Symposium on Solid Oxide Fuel Cells; 2003 April 27 – May 2; Paris, France. p. 105–112.

[6] Sfeir J, Mai A, Iwanschitz B, Weissen U, Denzler R, Haberstock D, et al. Status of SOFC stack and material development at Hexis. Proceedings 8th European SOFC Forum, Section B03, Industrial Experience [abstract 230, poster presentation]; 2008 July; Lucerne, Switzerland.

[7] Åström K, Fontell E, Virtanen S. Reliability analysis and initial requirements for FC systems and stacks. Journal of Power Sources 2007;171:46–54.

[8] Blum L, Packbier U, Vinke IC, de Haart LGJ. Long-term testing of SOFC stacks at Forschungszentrum Jülich. Fuel Cells 2013;13:646–653.

[9] Pohjoranta A, Halinen M, Pennanen J, Kiviaho J. Multivariable linear regression for SOFC stack temperature estimation under degradation effects. Journal of The Electrochemical Society 2014;161:F425–F433.

[10] Marseguerra M, Zio E, Cipollone M. Designing optimal degradation tests via multi-objective genetic algorithms. Reliability Engineering and System Safety 2003;79:87–94.

[11] Yuan X-X, Pandey MD. A nonlinear mixed-effects model for degradation data obtained from in-service inspections. Reliability Engineering and System Safety 2009;94:509–519.

[12] Kim S-J, Bae SJ. Cost-effective degradation test plan for a nonlinear random-coefficients model. Reliability Engineering and System Safety 2013;110:68–79.

[13] Micea MV, Ungurean L, Carstoiu GN, Groza V. Online state-of-health assessment for battery management systems. IEEE Transactions on Instrumentation and Measurement 2011;60:1997–2006.

[14] Bae SJ, Kim SJ, Um SK, Park JY, Lee JH, Cho H. A prediction model of degradation rate for membrane electrode assemblies in direct methanol fuel cells. International Journal of Hydrogen Energy 2009;34:5749–5758.

[15] Xing Y, Ma EWM, Tsui KL, Pecht M. An ensemble model for predicting the remaining useful performance of lithium-ion batteries. Microelectronics Reliability 2013;53:811–820.

[16] Guida M, Postiglione F, Pulcini G. A time-discrete extended Gamma process for time-dependent degradation phenomena. Reliability Engineering and System Safety 2012;105:73–9.

[17] Nelson W. Accelerated Testing: Statistical Models, Test Plans and Data Analyses. New York: John Wiley & Sons; 1990.

[18] Vonesh EF and Chinchilli VM. Linear and Nonlinear Models for the Analysis of Repeated Measurements. New York: Marcel Dekker; 1997.

[19] Demidenko E. Mixed Models: Theory and Applications with R. 2nd ed. New York: John Wiley & Sons; 2013.

[20] Montgomery DC, Jennings CL, Kulahci M. Introduction to Time Series Analysis and Forecasting. Hoboken (NJ): John Wiley & Sons; 2008.

[21] Box GEP, Jenkins GM, Reinsel GC. Time Series Analysis: Forecasting and Control. 4th ed. Hoboken (NJ): John Wiley & Sons; 2008.

[22] Draper NR, Smith H. Applied Regression Analysis. 3rd ed. New York: John Wiley & Sons; 1998.

[23] Amemiya Y. What should be done when an estimated between group covariance matrix is non-negative definite. The American Statistician 1985;39:112–7.

[24] R-project.org [Internet]. R Development Core Team. R: a language and environment for statistical computing. Vienna: R Foundation for Statistical Computing; 2014 [cited 2014 Dec 31]. Available from: http://www.R-project.org/ .

[25] Mood AM, Graybill FA. Introduction to the theory of statistics. New York: McGraw-Hill; 1963.

Appendix A

The result that $\mathbf{\Sigma}_{\hat{\mathbf{B}}} = \mathbf{\Sigma}_{\mathbf{B}} + \mathbf{\Sigma}_{\hat{\mathbf{B}}|\mathbf{B}}$ stems from the fact that

$$\begin{aligned}\mathbf{\Sigma}_{\hat{\mathbf{B}}} &\equiv E\left\{\left[\hat{\mathbf{B}}_i - E(\hat{\mathbf{B}}_i)\right]\left[\hat{\mathbf{B}}_i - E(\hat{\mathbf{B}}_i)\right]^T\right\} = \\ &= E_{\mathbf{B}}\left\{\left[E_\varepsilon\left(\hat{\mathbf{B}}_i|\mathbf{B}_i\right) - E_{\mathbf{B}}\left\{E_\varepsilon\left(\hat{\mathbf{B}}_i|\mathbf{B}_i\right)\right\}\right]\left[E_\varepsilon\left(\hat{\mathbf{B}}_i|\mathbf{B}_i\right) - E_{\mathbf{B}}\left\{E_\varepsilon\left(\hat{\mathbf{B}}_i|\mathbf{B}_i\right)\right\}\right]^T\right\} + \\ &\quad E_{\mathbf{B}}\left\{E_\varepsilon\left\{\left[\hat{\mathbf{B}}_i - E_\varepsilon\left(\hat{\mathbf{B}}_i|\mathbf{B}_i\right)\right]\left[\hat{\mathbf{B}}_i - E_\varepsilon\left(\hat{\mathbf{B}}_i|\mathbf{B}_i\right)\right]^T|\mathbf{B}_i\right\}\right\}\end{aligned}$$

Since, however $E_\varepsilon\left(\hat{\mathbf{B}}_i|\mathbf{B}_i\right) = \mathbf{B}_i$, $E_{\mathbf{B}}\left\{E_\varepsilon\left(\hat{\mathbf{B}}_i|\mathbf{B}_i\right)\right\} = E(\mathbf{B}_i) = \boldsymbol{\mu}_{\mathbf{B}}$, and by recalling the assumption of a common covariance matrix across units, it follows that

$$\mathbf{\Sigma}_{\hat{\mathbf{B}}} = \mathbf{\Sigma}_{\mathbf{B}} + E_{\mathbf{B}}\left(\mathbf{\Sigma}_{\hat{\mathbf{B}}|\mathbf{B}}\right) = \mathbf{\Sigma}_{\mathbf{B}} + \mathbf{\Sigma}_{\hat{\mathbf{B}}|\mathbf{B}}.$$

Appendix B

In order to compute an interval estimate of $R(x)$, we recast (16) as

$$\hat{R}(x) = \Phi\left\{\sqrt{n-1}\sqrt{\frac{\mathbf{x}^T\mathbf{\Sigma}_{\mathbf{B}}\mathbf{x}}{(n-1)\mathbf{x}^T\hat{\mathbf{\Sigma}}_{\mathbf{B}}\mathbf{x}}}\left[\Phi^{-1}\left[R(x)\right] + \frac{1}{\sqrt{n}}\frac{\sqrt{n}\left(\hat{\boldsymbol{\mu}}_{\mathbf{B}}^T\mathbf{x} - \boldsymbol{\mu}_{\mathbf{B}}^T\mathbf{x}\right)}{\sqrt{\mathbf{x}^T\mathbf{\Sigma}_{\mathbf{B}}\mathbf{x}}}\right]\right\} \qquad \text{(B.1)}$$

and observe that, in absence of noise, $\hat{\boldsymbol{\mu}}_{\mathbf{B}}^T\,\mathbf{x}$ and $\mathbf{x}^T\hat{\mathbf{\Sigma}}_{\mathbf{B}}\mathbf{x}$ coincide with the conventional unbiased estimates of the mean and variance of a normal variable, based on *n* independent realizations. Thus,

in repeated sampling, $(n-1)\left(\mathbf{x}^T\hat{\boldsymbol{\Sigma}}_{\mathbf{B}}\mathbf{x}\right)/\left(\mathbf{x}^T\boldsymbol{\Sigma}_{\mathbf{B}}\mathbf{x}\right)$ and $\sqrt{n}\left(\hat{\boldsymbol{\mu}}_{\mathbf{B}}^T\mathbf{x}-\boldsymbol{\mu}_{\mathbf{B}}^T\mathbf{x}\right)/\sqrt{\mathbf{x}^T\boldsymbol{\Sigma}_{\mathbf{B}}\mathbf{x}}$ are pivotal quantities, distributed as a chi-squared r.v. with $\nu = n-1$ d.o.f., and a Standard Normal Z r.v., respectively. Hence, equation (B.1) can be re-written as

$$\hat{R}(x) = \Phi\left\{\sqrt{(n-1)/\chi^2_{n-1}}\left[\Phi^{-1}\left[R(x)\right]+Z/\sqrt{n}\right]\right\}, \tag{B.2}$$

showing that the sampling distribution of the estimator $\hat{R}(x)$ depends on the sample size n, and on the unknown model parameters only through the true reliability $R(x)$.

This allows one to construct approximate confidence intervals on $R(x)$ through an iterative procedure that adopts the Monte Carlo method to obtain the sampling distribution of $\hat{R}(x)$, for given $R(x)$ and n. The procedure is outlined below:

Step 1 - On the basis of the estimates $\hat{\boldsymbol{\mu}}_{\mathbf{B}}$ and $\hat{\boldsymbol{\Sigma}}_{\mathbf{B}}$, compute the point estimate of the item reliability at time x, say $\hat{R}$, by (16);

Step 2 - Set an initial guess of the true reliability at x, say R, and use Monte Carlo method and equation (B.2) to generate N_S pseudo-random realizations of the estimator (16);

Step 3 - Order this sample, and compute the upper $1-\alpha$ (lower α) quantile, say $\hat{R}_{1-\alpha}$ ($\hat{R}_{\alpha}$), of the empirical distribution of $\hat{R}$ as described in [25];

Step 4 - Compare the quantile $\hat{R}_{1-\alpha}$ ($\hat{R}_{\alpha}$) to $\hat{R}$. If $R_{1-\alpha} \neq \hat{R}$ ($R_{\alpha} \neq \hat{R}$), iteratively change the value of R and repeat steps 2 and 3 until convergence is reached. The value of R at convergence represents the lower (upper) bound of the $1-2\alpha$ confidence interval on the reliability at time x.

Actually, in order to avoid numerical drawbacks occurring in correspondence of very high (very low) reliability values, the above procedure is used to obtain the confidence interval on the quantity $\Phi^{-1}(R(x))$ on the basis of the sampling distribution of the r.v. $W = \Phi^{-1}(\hat{R})$, and then transforming this interval into the confidence interval on $R(x)$.

It is to be noted, however, that in presence of noise, the distributional results in (B.2) do not hold exactly, for the estimates $\hat{\boldsymbol{\mu}}_{\mathbf{B}}^{T}\,\mathbf{x}$ and $\mathbf{x}^{T}\hat{\boldsymbol{\Sigma}}_{\mathbf{B}}\mathbf{x}$ are affected by an increased sampling variability due to the presence of noise. This effect, however, should tend to decrease asymptotically (as $m \to \infty$), so that in the case studies analysed in this paper we can reasonably assume that equation (B.2) is approximately true, and hence we construct approximate confidence intervals for the reliability function as described above.

Table 1. Case study A: OLS estimates of regression parameters for each cell, their mean and standard deviation over the cells, and the coefficient of determination

	$\hat{B}_{0i}$	$\hat{B}_{1i}$	$\hat{B}_{2i}$	$\hat{B}_{3i}$	R_i^2
Cell 1	0.188765	-0.027651	0.037759	-0.030708	0.995
Cell 2	0.188663	-0.041010	0.073653	-0.057346	0.993
Cell 3	0.187663	-0.037286	0.079173	-0.071681	0.995
Cell 4	0.184942	-0.031351	0.051944	-0.050941	0.997
Sample Mean	0.187508	-0.034324	0.060632	-0.052669	
Sample St. Dev.	0.001781	0.005968	0.019253	0.017016	

Table 2. Case study A: Estimates of noise variance for each cell, and its pooled estimate

	s_i^2
Cell 1	1.19429E-07
Cell 2	1.72146E-07
Cell 3	1.95555E-07
Cell 4	1.42849E-07
Pooled estimate s^2	1.57495E-07

Table 3. Case study B: OLS estimates of regression parameters for each cell, their mean and standard deviation, and the coefficient of determination

	$\hat{B}_{0i}$	$\hat{B}_{1i}$	$\hat{B}_{2i}$	$\hat{B}_{3i}$	R_i^2
Cell 1	0.192299	-0.018925	0.045986	-0.048372	0.958
Cell 2	0.189773	-0.018090	0.041007	-0.046342	0.965
Cell 3	0.191700	-0.009754	0.011825	-0.021579	0.954
Cell 4	0.192600	-0.026780	0.053129	-0.052486	0.957
Cell 5	0.192396	-0.008727	0.010622	-0.023290	0.979
Sample Mean	0.191754	-0.016455	0.032514	-0.038414	
Sample St. Dev.	0.001157	0.007416	0.019912	0.014766	

Table 4. Case study B: Estimates of noise variance for each cell, and its pooled estimate

	s_i^2
Cell 1	2. 22710E-07
Cell 2	2.65702E-07
Cell 3	4.06065E-07
Cell 4	3.98107E-07
Cell 5	2.00316E-07
Pooled estimate s^2	3.10481E-07

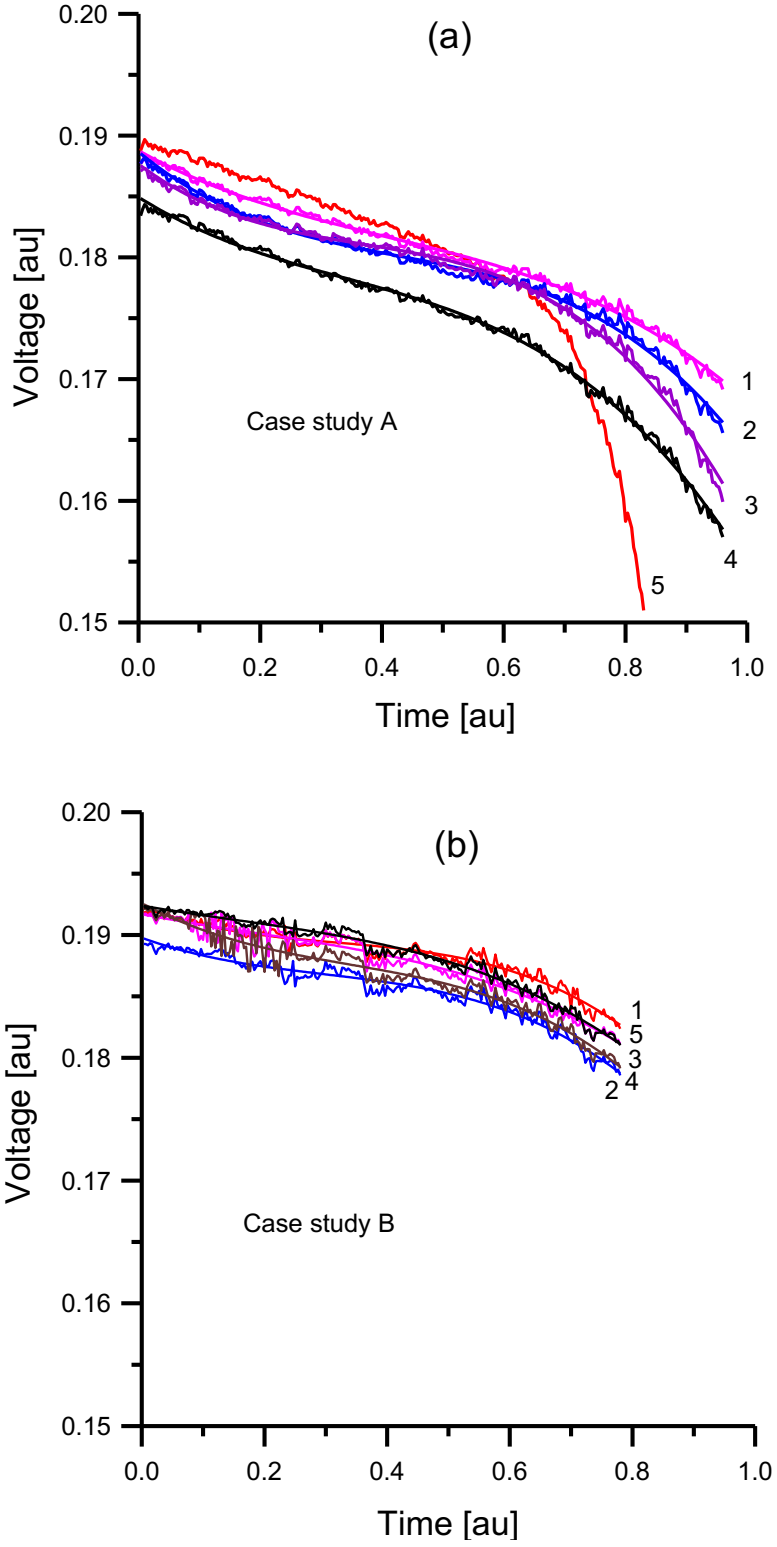

Fig. 1. Observed cell voltage vs. time in arbitrary units (au), and the corresponding estimated empirical models (see Section 3.1) for cells of case studies A (a) and B (b).

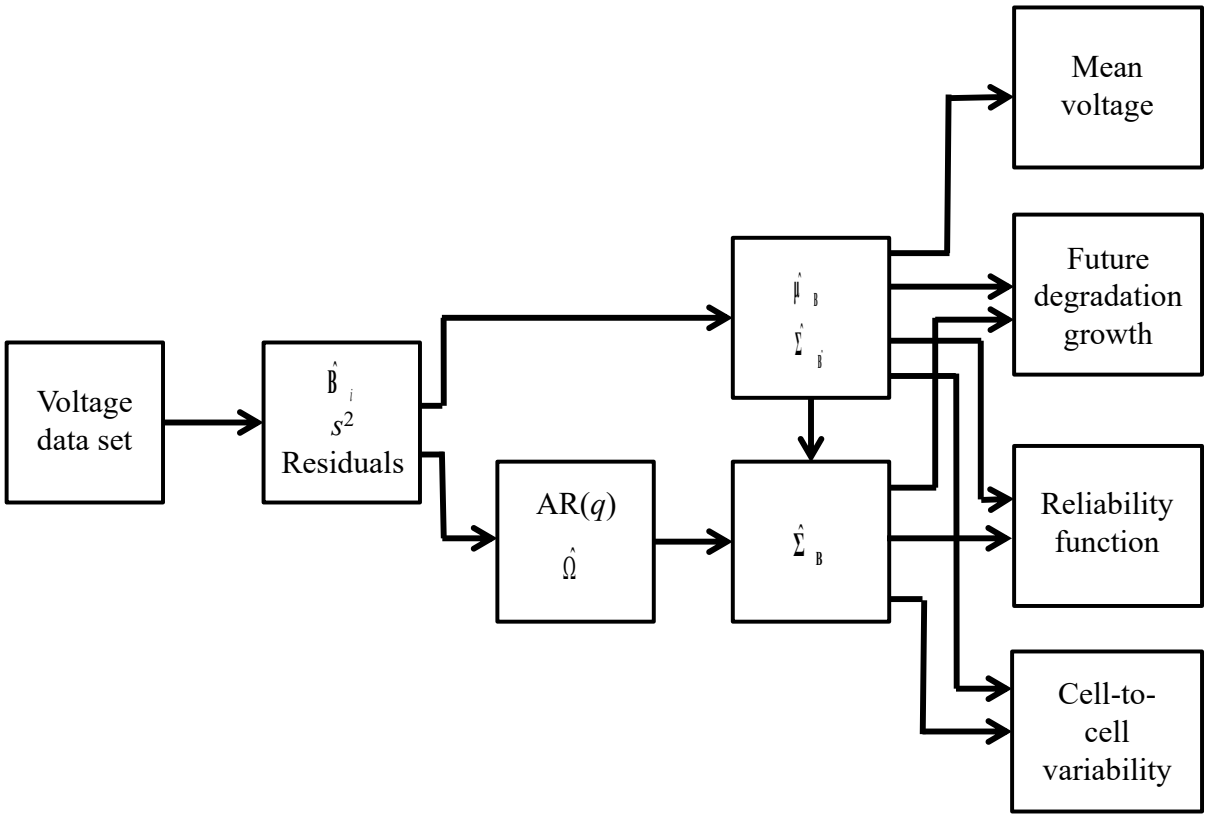

Fig. 2. Flow diagram of the estimation procedure.

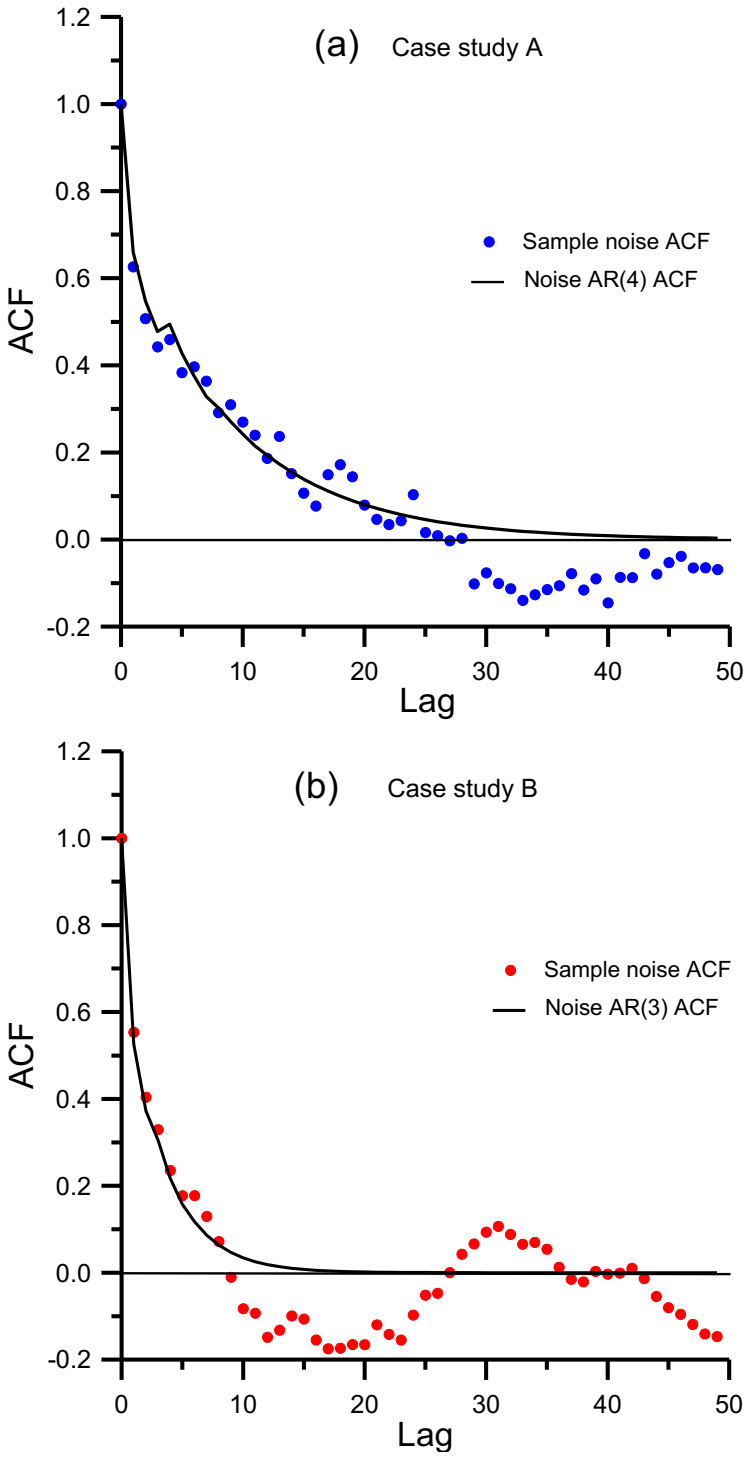

Fig. 3. Averaged sample noise ACF and noise AR(q) ACF for case studies A (a) and B (b).

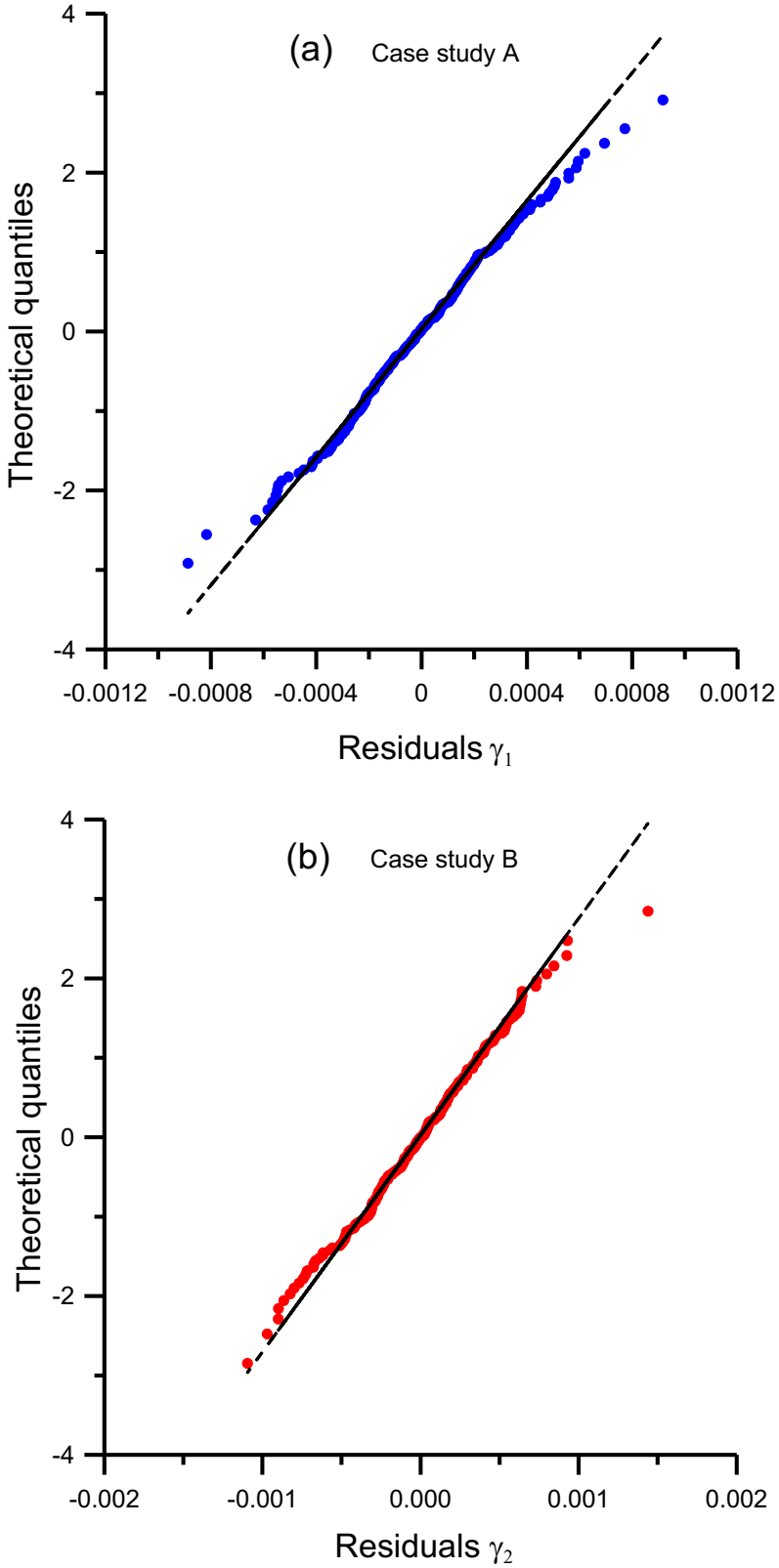

Fig. 4. Normal probability plot of residuals γ of cell no. 1 in case study A (b), and of cell no. 2 in case study B (b).

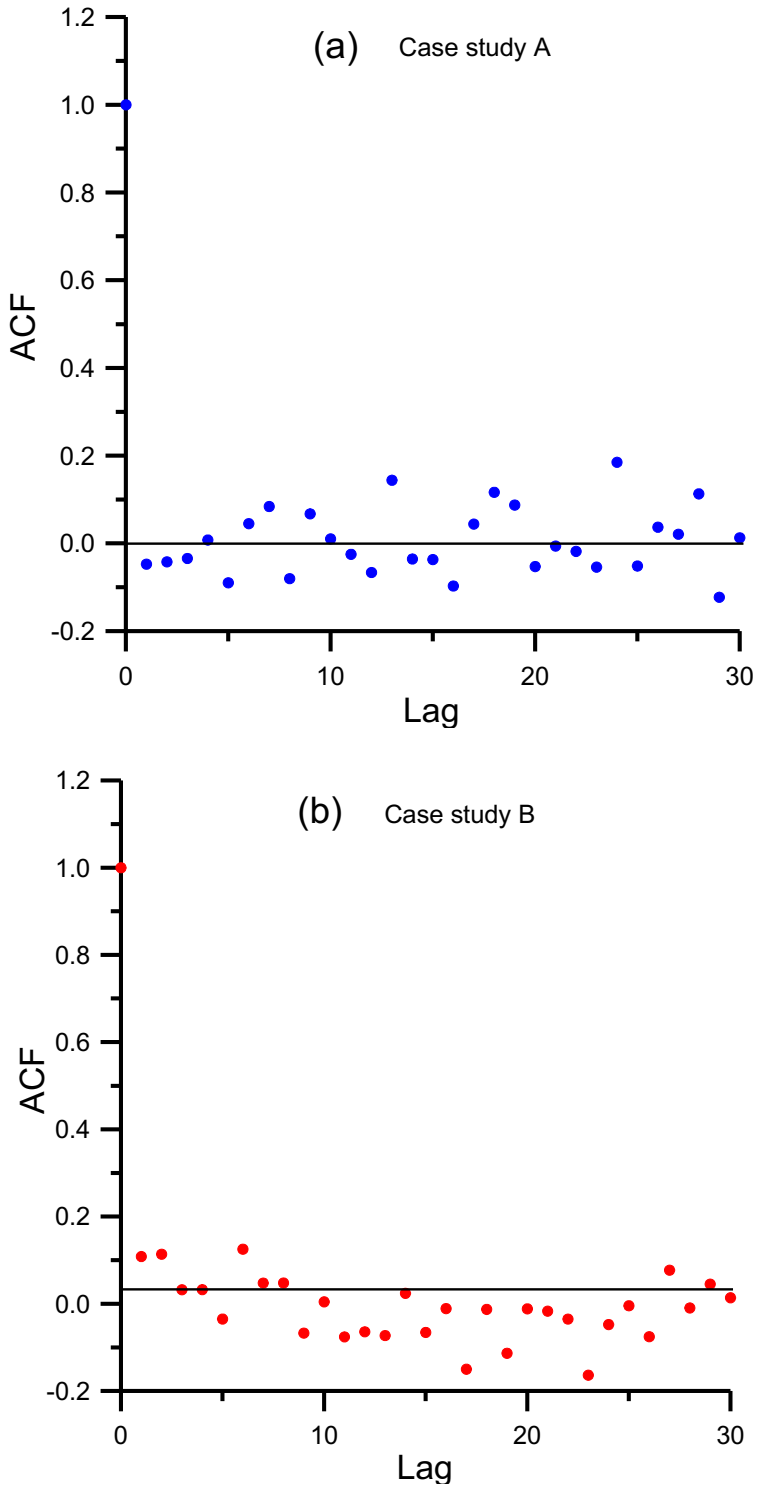

Fig. 5. Autocorrelation function of residuals γ of cell no. 1 in case study A (b), and of cell no. 2 in case study B (b).

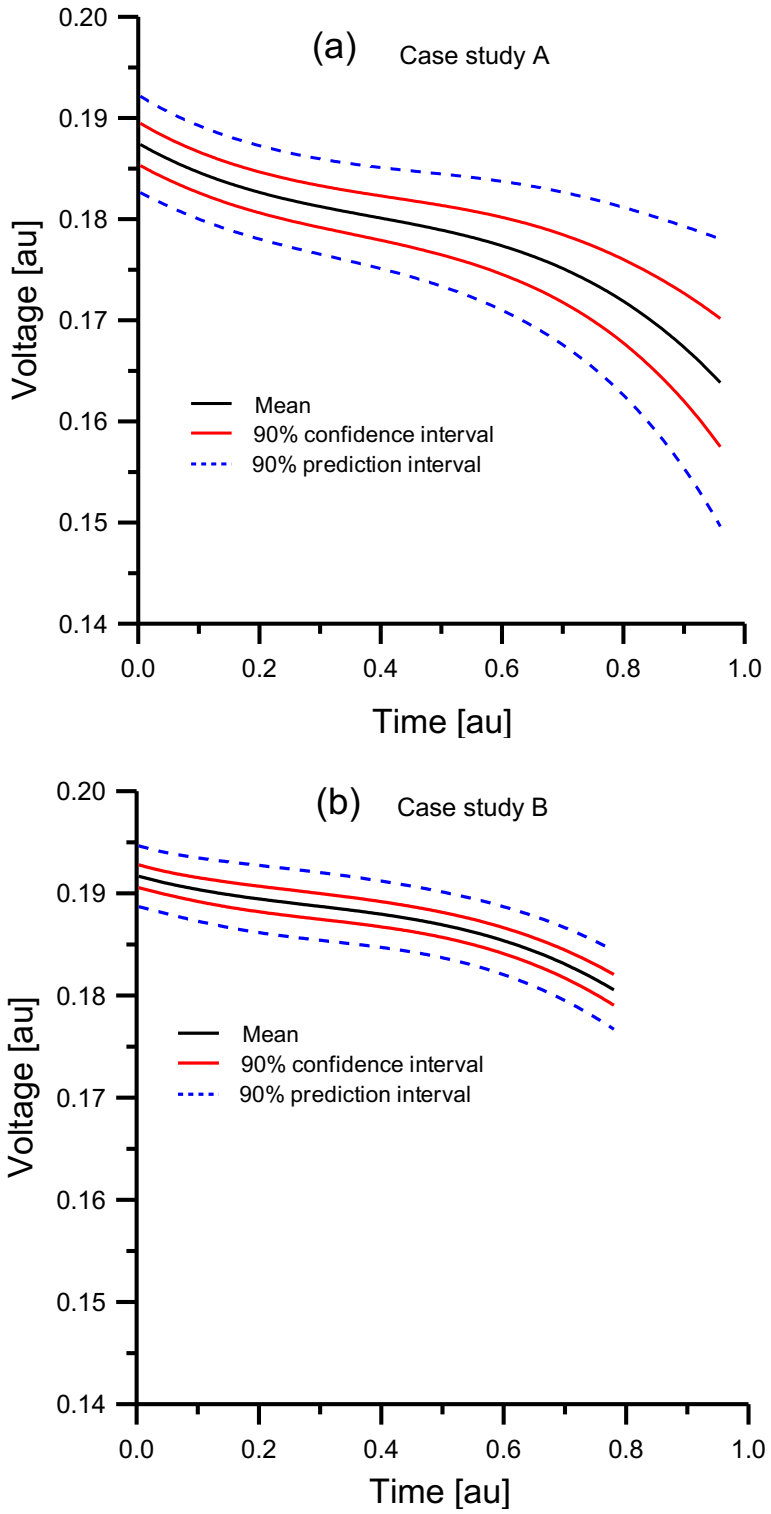

Fig. 6. 90% confidence interval for the mean voltage and 90% prediction interval for case studies A (a) and B (b). Both voltage and time are in arbitrary units (au).

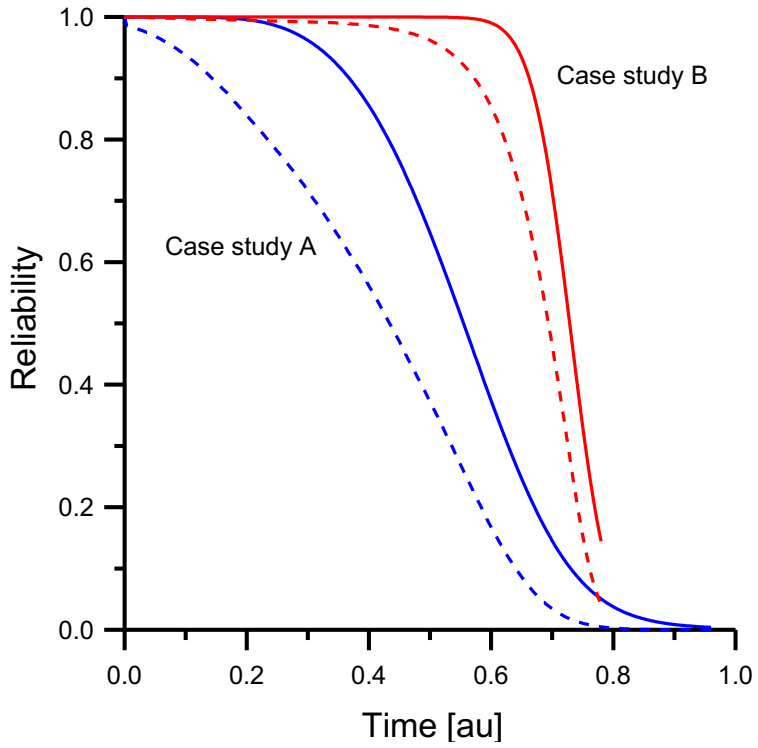

Fig. 7. Point estimate (——) and 90% lower confidence limit (- - -) of the reliability function for case studies A and B.

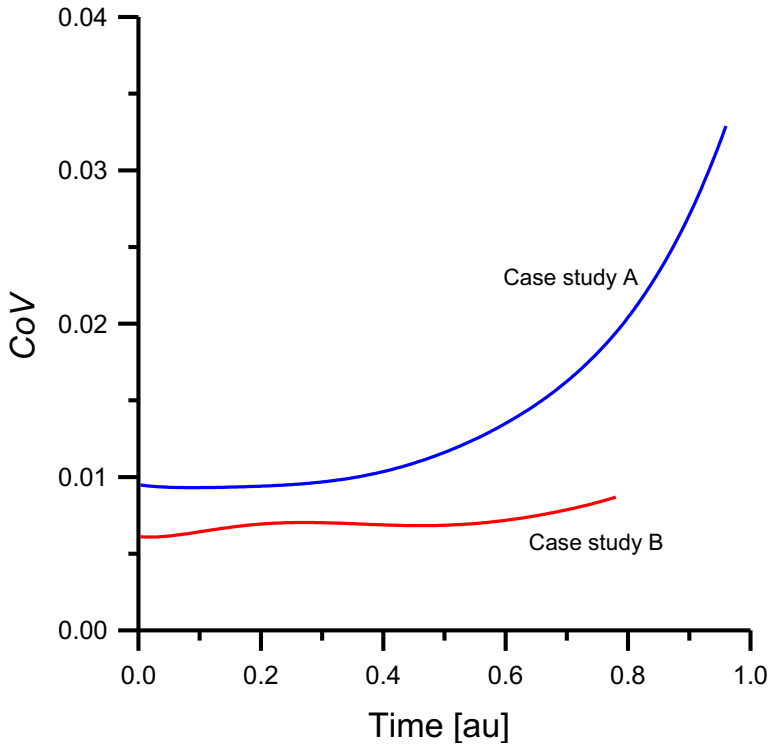

Fig. 8. Estimates of cell-to-cell variability for case studies A and B in terms of the coefficient of variation of $Y(x)$.